6

CHAPTER 6: MODELLING AND OPTIMISATION OF COOLING CHANNEL GEOMETRIC CONFIGURATION FOR OPTIMAL THERMAL PERFORMANCE OF A PROTON EXCHANGE MEMBRANE FUEL CELL

6.1 INTRODUCTION

A fuel cell is an electrochemical energy device that directly converts the chemical energy in the fuel into electrical energy. Applications include: portable power, stationary applications, vehicle propulsion and large electrical plants. PEM fuel cell researchers are moving ahead at a rapid pace because of the many attractive features, like rapid start-up, high power density, high efficiency and the belief of being the most promising among fuel cell types for transportation application, due to its fast start-up and dynamic response to changes in the demand for power during vehicular operations [71, 220, 221]. These features have made it one of the most promising clean and highly efficient power generation technologies in the 21st century. Operating temperatures of fuel cell systems affect the maximum theoretical voltage at which a fuel cell can operate [89]. Higher operating temperatures correspond to lower theoretical maximum voltages and lower theoretical efficiency. However, higher temperature at fuel cell electrodes increases electrochemical activity which, in turn, increases efficiency [89]. Most current PEM fuel cells operate at low temperatures (< 80^{o}C) encountering several performance difficulties, especially vehicular applications such as reduced electrochemical kinetics at electrode sites; flooding due to two-phase flows emergence; intolerance to impurities such as CO; insufficient heat rejection capability and relatively high cost. A recent approach is to operate this class of fuel cell at higher temperature (> 100^{o}C) which eliminates some of these obstacles [88,

222-224]. Operating at higher temperatures increases the reaction rates at both electrodes and consequently increases system efficiency. The quality of waste heat from the fuel cell stack, which could be used in other system components requiring heat or used to run an additional thermodynamic heat for additional power, is also enhanced at higher operating temperature. Also, there is a substantial reduction in the incidence of water "flooding" that restricts oxygen transport by blocking the channel path and pores of the gas diffusion electrodes when fuel cells are operated at a higher temperature. Several approaches are also on-going, especially on developing PEM materials (polymers, catalyst layers and MEA compositions) that will be relatively stable for compatibility with operation at high temperatures [104, 225, 226]. The development of these materials comes with an additional cost of operating a PEM fuel cell.

Moderate temperature ranges exist within which a specific fuel cell type will operate efficiently and reliably. Subsequently, the goal in fuel cell thermal management is to ensure effective stack operation at a specified temperature range. A PEMFC operated at 80^{o}C with an efficiency of 40-50% produces an enormous amount of heat (~ 50% waste heat) due to the exothermic nature of the cell reaction that must be removed if the integrity of the cell structure is to be maintained [222]. In a typical modern vehicle based on the internal combustion engine (ICE), the cooling system rejects < 40% of the generated waste heat and the exhaust manifold removes the bulk of the waste heat in the system [227]. In contrast, a typical PEM fuel cell stack operating at 80^{o}C must reject all the heat produced via the cooling system.

The heat rejection capability of a PEM fuel cell system operating below 100^{o}C is very inefficient and requires elaborate cooling systems for adequate system performance [88]. Basically, cooling methods are predominantly determined by the size of the fuel cell system [119]. The size of the fuel cell system also has a direct link with the required power output from the fuel cell system. Fuel cell units below 2 kW are better cooled using air, while systems between 2 kW and 10 kW require judicious decision-making to use water or air cooling [89]. Water cooling requires more complex system

design when considering the need to monitor the temperature and pressure of the cooling water and the need for an oil-free water pump to supply cooling water. Air cooling could be achieved through increasing the reactant air flow to the fuel cell system but with the risk of too much air drying out the PEM [119]. This associated problem usually necessitates the use of a separate reactant air supply and a cooling system for the fuel cell system.

Temperature distribution in fuel cells is usually non-uniform, even when there is a constant mass flow rate in the flow channels [228]. This occurs primarily as a result of the heat transfer and phase changes in PEM fuel cells. It usually causes temperature fluctuations within the fuel cell system structure and affects the fuel cell performance. Heat transfer in PEM fuel cells occurs in the following ways [228]:

- Between the cell component layers and the flowing air and fuel streams. This way of heat transfer is usually described in terms of heat transfer coefficients h_a (for air channel) and h_f (for fuel channel) due to forced convective heat transfer with or without natural convection.
- Between the fuel and air streams across the interconnect layer, described as overall heat transfer coefficient, *U;*
- In solid structures, described as heat conduction with different thermal conductivities, k_i ($i =$ electrolyte, electrodes and current interconnect layers).

In order to alleviate the excessive temperature build-up in a PEM fuel cell, the heat generated by the various processes in the fuel cell structure should be removed properly. Thermal management has a very strong impact on fuel cell performance, since it affects the transport of water and gaseous species as well as electrochemical reactions in the cells. Thermal management still remains a critical issue that needs to be resolved in order for PEM fuel cell technology to be feasible for various commercial applications [229, 230]. A number of numerical modelling works has been carried out in the literature to investigate heat/mass transfer in PEM fuel cells.

Yu *et al.* [98] investigated the performance of the Ballard PEM fuel cell in terms of electrochemical characteristics and water management. The study shows that the more the water supplied to the anode from its inlet, the higher the voltage and usually the lower the anode exit temperature. Coppo *et al.* [90] presented a 3-D model to study the influence of temperature on PEM fuel cell operation which includes a two-phase flow in the gas distribution channel. The obtained result indicates that both liquid water transport within the GDL and liquid water removal from the surface of the GDL play an important role in determining variations in cell performance as far as temperature is concerned.

Yan *et al.* [91] presented a 1-D non-isothermal model to analyse the effect of anode and cathode side temperatures on the membrane water distribution. The obtained results shows that a temperature increase on the anode side can lead to membrane dehydration and fuel cell operation at high current density leads to membrane dehydration on the anode side, due to the strong electro-osmotic water drag at high current density. Ramousse *et al.* [92] developed a 1-D non-isothermal model accounting for heat and mass transfer in a complete cell with charge and mass transfer in the electrodes. Their study provides temperature, concentration and potential fields in a single cell. In addition, their work shows that the thermal gradient in MEA could lead to thermal stresses at high current densities.

Shimpalee and Dutta [93] conducted a 3-D non-isothermal numerical analysis with a two-phase flow phenomenon incorporated in their model. The effect of the heat produced by the electrochemical reaction and phase change of water on the cell performance was studied critically. Their study shows that the inclusion of heat transfer in fuel cell model shows degradation in fuel cell performance. This research work enumerated the importance of incorporating the heat transfer aspect in fuel cell modelling. Shan and Choe [94] presented a 1-D model taking into account the dynamics in temperature gradient across the fuel cell; the dynamics in water concentration redistribution in the membrane; the dynamics in proton concentration in the cathode catalyst layer; and the dynamics in reactant concentration redistribution in

the cathode GDL. This study's general result shows that temperature profiles in each of the cell layers tend to follow the current waveform due to energy losses in these layers. Higher temperature losses are prominent in the membrane and catalyst layer due to ohmic losses as a result of the membrane resistance and heat released by the chemical reaction.

Yuan and Sunden [95] performed a 3-D non-isothermal numerical analysis of heat transfer and gas flow in PEM fuel cell ducts using a generalised extended Darcy model. The effects of effective thermal conductivity, permeability, inertia coefficient and porous layer thickness on gas flow and heat transfer were studied. Their result shows that higher permeability, higher effective thermal conductivity of porous GDL and smaller thickness of the porous layer improved heat transfer in the modelled fuel cell system. Ju *et al.* [96] presented a 3-D non-isothermal single-phase model for all seven layers of the PEM fuel cell that accounts for various location-specific heat-generation mechanisms. These mechanisms include irreversible heating due to electrochemical reactions and entropy, and Joule (ohmic) heating due to membrane ionic resistance. They observed that the thermal effect on PEM fuel cells becomes more critical at higher cell current density and/or lower GDL thermal conductivity. Their result further shows that temperature increase in the membrane is highly dependent on the GDL thermal conductivity and inlet humidity conditions.

A number of modelling approaches has been developed in the literature to predict the thermal effect in PEM fuel cells as described above [90, 98, 91-96] but, although they represent a significant contribution in fuel cell thermal modelling, there are few reports on thermal cooling approaches to enhance thermal management in a PEM fuel cell structure. Furthermore, most models on thermal management in PEM fuel cells emphasise approaches to understand and improve the kinetic process for thermal prediction aimed at improving individual fuel cell model performance, rather than a practical approach to reduce the incident temperature generated in the fuel cell structure. One of the enhancement techniques to reduce excessive temperature build-

up in a PEM fuel cell is by using air/water (depending on fuel cell size) cooling, conveyed through cooling channels, as an integral part of the fuel cell flow structure.

To the author's knowledge, studies on the impact of the geometric configuration of cooling channels on effective thermal heat transfer and performance in the fuel cell system is still limited in the literature and this phenomenon is explored in this study. A numerical modelling study that investigates the geometrical effect of cooling channels on the thermal performance of a PEM fuel cell is described in this chapter. A parametric study on the effect of temperature, stoichiometry ratio, relative humidity and the cooling channel aspect ratio on cell performance were initially conducted, since these factors contribute to the extent of membrane hydration in a fuel cell system. Optimal results of these parameters were subsequently combined with the different aspect ratio of the cooling channels and the system performance was evaluated for elevated fuel cell system temperatures (100-150°C). In addition, a mathematical optimisation tool was used to select the best geometric configuration that would improve cooling and enhance fuel cell performance for a given cooling gas flow Reynolds number. The results of this study will be of interest to fuel cell engineers who are striving to improve thermal management in fuel cell systems and enhance system performance.

6.2 MODEL DESCRIPTION

In this chapter, a numerical study and optimisation of geometric parameters of the cooling channel of a PEM fuel cell is attempted, based on a three-dimensional full cell model, and the impact on cell performance is explored. The single-cell PEMFC consists of the anode flow channel, anode diffusion layer, MEA assembly, cathode diffusion layer, cathode flow channel, as well as an array of cooling channels on the carbon plates. Figure 6.1 shows the 3-D schematic of the model of the PEM fuel cell system. The influential factors considered in this study that could affect the fuel cell thermal behaviour and subsequently performances are the stoichiometry ratio, the

relative humidity, the cooling channel aspect ratio and the coolant air Reynolds number. The construct of three (3) cooling channels transversely placed at equal distances at each side (anode and cathode) of the bipolar plates of the PEM fuel cell are shown in Figure 6.1. These parameters are selected as the design parameters to be optimised in this study. The other geometric and physicochemical properties for the fuel cell system are kept constant in this study and given in Table 6.1.

The Dynamic-Q optimisation algorithm [166] is employed herein as the optimisation search scheme. This study is aimed at optimising these identified factors, so that the best performance in terms of the optimal current density (the objective function) of the PEM fuel cell system at prescribed operating conditions can be achieved. The optimisation algorithm is expected to ensure robust optimal values for the factors investigated in this study.

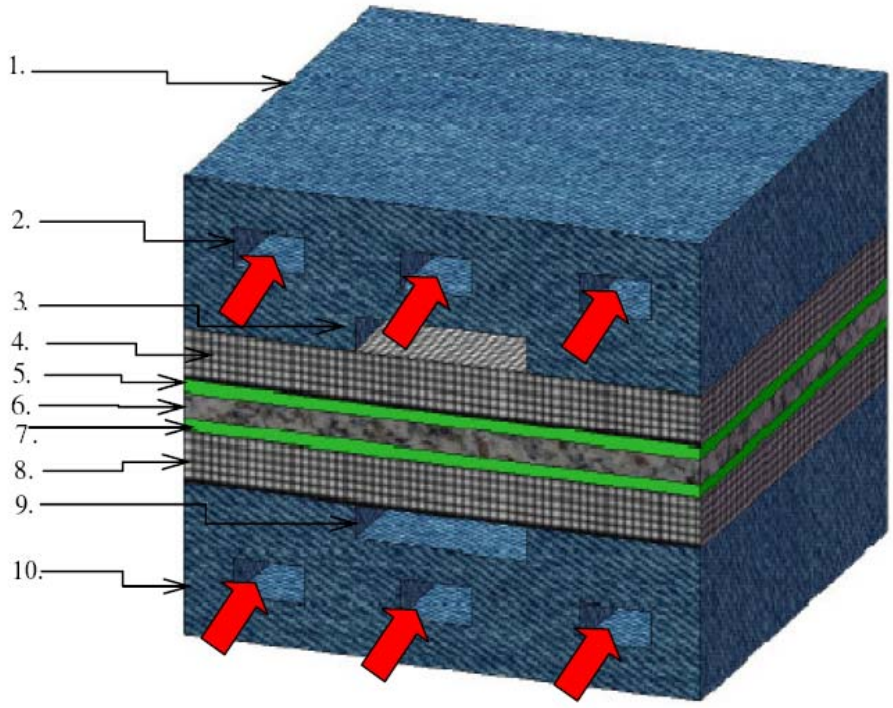

Figure 6.1 A schematic diagram of a 3-D model of PEM fuel cell system with cooling channels embedded in the bipolar plates

1. Anode-side bipolar plate
2. Cooling channel
3. Hydrogen fuel channel
4. Anode GDL
5. Anode catalyst layer
6. Membrane
7. Cathode catalyst layer
8. Cathode GDL
9. Air gas channel
10. Cathode-side bipolar plate

Table 6.1 Parameters and properties used in the present model

Description	Value
Cell operating temperature (^{o}C)	70
Air-side/fuel-side inlet pressure (atm)	3/3
Open-circuit voltage (V)	0.95
Porosity of GDL	0.4
Permeability of GDL (m^2)	1.76×10^{-11}
Tortuosity of GDL	1.5
Porosity of catalyst layer	0.4
Permeability of catalyst layer (m^2)	1.76×10^{-11}
Tortuosity of catalyst layer	1.5
Porosity of membrane	0.28
Permeability of membrane (m^2)	1.8×10^{-18}
Reference diffusivity of H_2	0.915×10^{-4} m^2 s^{-1}
Reference diffusivity of O_2	0.22×10^{-4} m^2 s^{-1}
Electric conductivity of catalyst layer $(\Omega^{-1}m^{-1})$	190
Electric conductivity of GDL $(\Omega^{-1}m^{-1})$	300
Electric conductivity in carbon plate $(\Omega^{-1}m^{-1})$	4000

O_2 stochiometry ratio	1.2
H_2 stochiometry ratio	2.0
Oxygen mole fraction	0.406
Relative humidity of inlet fuel/air	100%
Reference current density of anode	7 500
Reference current density of cathode (A/m^2)	20
Anode transfer coefficient	0.5
Cathode transfer coefficient	0.5
Evaporation and condensation rate	100 s^{-1}

6.2.1 BASIC ASSUMPTIONS

The electrochemical reactions in the fuel cell are complicated, hence the following simplifying assumptions are made:

1. Ideal gas mixture in the flow channels and the porous electrode;
2. Incompressible and laminar flow;
3. Isotropic and homogeneous porous medium;
4. Ionic conductivity of both the membrane and catalyst layer are constant;
5. No pressure gradient between the anode and the cathode side (only gas diffusion is considered);
6. "ultra thin" electrode layer, hence gas transport resistance through the electrode porous layer could be neglected;
7. Identical inlet conditions for both the anode and cathode as well as the coolant channel;
8. No gas pressure drop along the gas channels;
9. Liner temperature gradient across the layers in the fuel cell;
10. Constant thermal conductivity of the materials in the fuel cell.

6.2.2 GOVERNING EQUATIONS

The employed governing equations are a single set applicable to all domains (flow channels, GDL and catalyst layer). This approach is based on the previous work of Um *et al.* [71]. The conservation equations of mass, momentum, species, proton, electron and energy are presented below:

Continuity equation:

$$\nabla \cdot (\rho \mathbf{u}) = 0 \tag{6.1}$$

Momentum:

$$\frac{1}{\varepsilon^2}\nabla \cdot (\rho \mathrm{uu}) = -\nabla p + \nabla \cdot \tau + S_u \tag{6.2}$$

Species:

$$\nabla \cdot (\mathbf{u} C_k) = \nabla \cdot (D_k^{eff} \nabla C_k) + S_k \tag{6.3}$$

Proton:

$$\nabla \cdot (\kappa^{eff} \nabla \Phi_e) + S_\Phi = 0 \tag{6.4}$$

Electron:

$$\nabla \cdot (\sigma_s^{eff} \nabla \Phi_s) + S_\Phi = 0 \tag{6.5}$$

Energy:

$$\nabla \cdot \left(\rho c_p \mathbf{u} T\right) = \nabla \cdot \left(k^{eff} \nabla T\right) + S_T \tag{6.6}$$

The energy source term, S_T, depicts the sum of the reversible heat release and the irreversible heat generation. In the catalyst layer, the reversible and irreversible reaction heats, as well as latent heat of water phase change, are considered. For the membrane, the ohm heating of the current due to the large resistance of the membrane is also considered. The detailed source terms used for the model in the equations above are presented in Table 6.2.

Table 6.2 The governing equation source terms in various regions of the fuel cell

	Gas channel	Diffusion layer	Catalyst layer	Membrane
Mass	$S_m = 0$	$S_m = 0$	Anode: $S_m = S_h + S_w$, Cathode: $S_m = S_o + S_w$,	$S_m = 0$
Momentum	$S_u = 0$	$S_u = -\frac{\mu_g}{k k_{rg}} \mathbf{u}_g$	$S_u = -\frac{\mu_g}{k k_{rg}} \mathbf{u}_g$	$S_u = 0$
Species:				
O_2	$S_o = 0$	$S_o = 0$	$S_o = -(i_c/4F)M_o$	$S_o = 0$
H_2	$S_h = 0$	$S_h = 0$	$S_h = -(i_a/2F)M_h$	$S_h = 0$
Charge:				
Solid phase -	$S_{\Phi,s} = 0$	$S_{\Phi,s} = 0$	$S_{\Phi,s} = -I$	$S_{\Phi,s} = 0$
Membrane phase-	$S_{\Phi,m} = 0$	$S_{\Phi,m} = 0$	$S_{\Phi,m} = I$	$S_{\Phi,m} = 0$

Energy	$S_T = 0$	$S_T = 0$	$S_T = i\left(\eta + T\frac{dV_{oc}}{dT}\right) + \frac{I^2}{\kappa_m}$ $S_T = \frac{I^2}{\kappa_m}$

The transfer current densities at the anode and the cathode are calculated using the Butler-Volmer equation [60]:

$$i_o = i_{o,ref}\left\{\exp\left[\frac{\alpha_{an} nF}{RT}\eta\right] - \exp\left[\frac{-\alpha_{cat} nF}{RT}\eta\right]\right\} \quad , \tag{6.7}$$

where η is the overpotential and defined as,

$$\eta = \left(\Phi_s - \Phi_e\right) - E_{ocv} \quad , \tag{6.8}$$

where F is the Faraday constant, α_{an} and α_{cat} represents the experimental anodic and cathodic transfer coefficients, respectively, and R is the universal gas constant. The effective diffusivity ($D_{i,eff}$) for the gas-phase flow in porous media can be written as:

$$D_{i,eff} = D\frac{\varepsilon}{\tau}. \tag{6.9}$$

The quantity (τ = tortuosity) is usually estimated through experiment. Therefore, it is conventionally correlated in fuel cell studies using the Bruggeman correlation [103]. This correlation assumes τ is proportional to $\varepsilon^{-0.5}$, resulting in the simpler expression [103]:

$$D_{i,eff} = D\varepsilon^{1.5}. \tag{6.10}$$

The porosity correlation is used to account for geometric constraints of the porous media.

The Reynolds number was defined as [205]:

$$\mathrm{Re} = \dot{m}D/(\mu A). \tag{6.11}$$

6.2.3 NUMERICAL PROCEDURE

The model equations were solved by using a finite-volume computational fluid dynamics code Fluent [163] with Gambit® (2.4.6) [164] as a pre-processor. The CFD code has an add-on package for fuel cells, which has the requirements for the source terms for species transport equations, heat sources and liquid water formations. The domain was discretised using a second-order discretisation scheme. The SIMPLE algorithm [192] for convection-diffusion analysis was utilised to deal with the pressure-velocity coupling. Numerical convergence was obtained at each test condition when the relative error of each dependent variable between two consecutive iterations was less than 1.0×10^{-7}. The domain was divided into hexahedral volume elements. A grid independence test was carried out to ensure that solutions were independent of the dimensions of the chosen grid with consideration for both accuracy and economics. For this purpose, five grid systems at 24 × 12 × 60, 34 × 12 × 60, 34 × 22 × 60, 44 × 22 × 60 and 34 × 34 × 60 were tested. The obtained results of the average current density under different grid systems, when the PEM fuel cell system operating voltage was 0.7 V, are summarised in Table 6.3. It was considered that the system of 34 × 22 × 60 (I = 1.7054 A/cm^2) was sufficient for the present study as a trade-off between accuracy and cost of time. A typical grid network for the computational domain is shown in Figure 6.2. The model and solution were implemented using an Intel® Core(TM) 2Duo 3.00 GHz PC with 3.24 GB of DDRam.

Table 6.3 Grid independence test

Grid size	I_{av} [A/cm^2]
24 × 12 × 60	1.7012
34 × 12 × 60	1.7048
34 × 22 × 60	1.7054

44 × 22 × 60	1.7055
34 × 34 × 60	1.7057

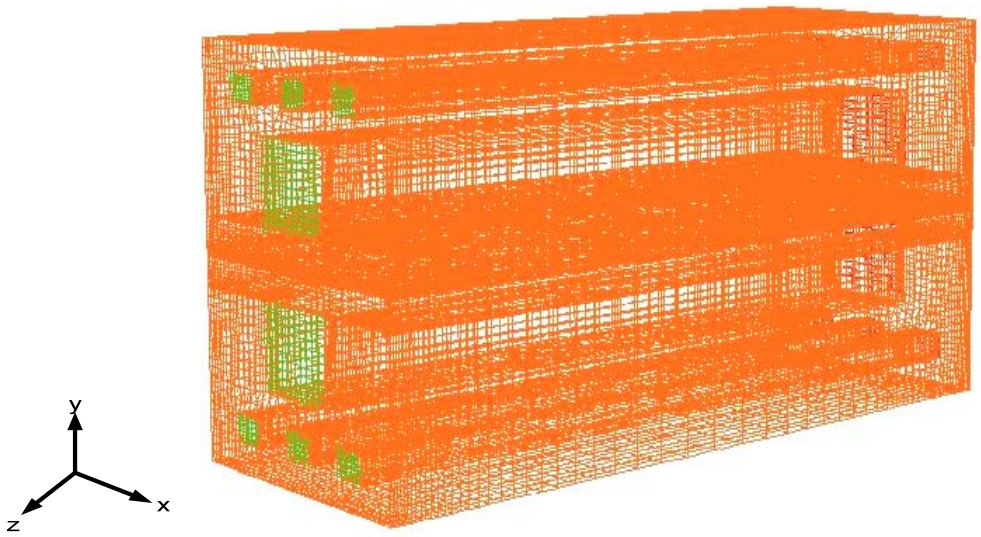

Figure 6.2 The discretised three-dimensional computational domain of a single PEM fuel cell with cooling channels

6.3 MATHEMATICAL OPTIMISATION ALGORITHM

The Dynamic-Q optimisation algorithm [166], previously discussed in detail in Chapter 3 of this thesis, was used in this study. The algorithm is a robust multidimensional gradient-based optimisation algorithm which does not require an explicit line search and is ideally robust for cases where function evaluations are computationally expensive. The algorithm applies the dynamic trajectory LFOPC which is adapted to handle constrained problems through approximate penalty function formulation [166]. This dynamic approach is applied to successive quadratic approximations of the actual optimisation problems. The successive sub-problems are formed at successive design points by constructing spherically quadratic approximations, which are used to approximate the objective functions or constraints (or both), if they are not analytically given or very expensive to compute numerically

[169, 207]. The use of spherical quadratic approximation in the Dynamic-Q algorithm offers a competitive advantage when compared with other algorithms in terms of the computational and storage requirements [169]. Storage savings become highly significant when the number of variables becomes large. Therefore, this particular strength of the Dynamic-Q method makes it well suited for optimisation of engineering problems with a large number of variables and it has been used to successfully solve a large variety of engineering problems [208, 210-213].

6.4 OPTIMISATION PROBLEM FORMULATION

The optimisation problem was tailored towards finding the best operating design parameters which would give the best performance in PEM fuel cells. The design variables which greatly affect the performance of PEM fuel cells, especially at high operating temperatures are the air stoichiometry ratio, relative humidity (*RH*), the aspect ratio of cooling channels and the coolant Reynolds number. The objective function here is the maximised current density of the fuel cell system at optimised operating factors (stoichiometry ratio, relative humidity, cooling channel aspect ratio and coolant Reynolds number) at a pressure drop of less than 3 atm. Table 6.4 shows the dimensions of the cooling channels used at base case condition for this study.

Table 6.4 Dimension of the cooling channels investigated for initial simulations

Test Case	W(mm)	H(mm)	L(mm)	$\alpha(=H/W)$
1	0.8	1.5	120	1.875
2	1.2	3.0	120	2.500
3	1.6	4.5	120	2.813

The objective function for the optimisation can be written mathematically as

$$I_{max} = f(\lambda_{opt}, RH_{opt}, H/W_{opt}, Re) \quad , \tag{6.12}$$

where I_{max} is the maximised current density output for the optimised design variables. The maximised current density approach in PEM fuel cell design has shown to be robust and allows the determination of maximum parameteric values that are sharp and robust enough for practical design applications [231]. In addition, when identified accurately they pave way for increasing the cell stack net power efficiency, approaching the actual PEMFC first-law efficiency level [231, 232]. The maximised current densities in this study were examined at the fuel cell voltage of 0.7V.

6.4.1 DESIGN VARIABLE CONSTRAINTS

Total fixed volume. For each of the optimisation problems, the cooling channel volume is kept constant.

The following constraints are imposed for the optimisation:

$$1 \leq \lambda \leq 5 \tag{6.13}$$

$$0.2 \leq RH \leq 1.0 \tag{6.14}$$

$$1.5 \leq H/W \leq 3.5 \tag{6.15}$$

$$100 \leq Re \leq 500 \tag{6.16}$$

6.4.2 OPTIMISATION PROCEDURE

The optimisation problem defined in Section 6.4.1 was automatically carried out in a MATLAB [218] environment by simultaneously using GAMBIT [164] for mesh generation and FLUENT [163] for modelling. This was made feasible by using both GAMBIT [164] and FLUENT [163] journal files, which were executed in MATLAB [218] by Windows executable files. Figure 6.3 depicts a flow diagram of how

automation is carried out until convergence (either by step size or function value criteria) is attained. To ensure that the converged solution obtained is indeed the global minimum, a multi-starting guess approach was employed.

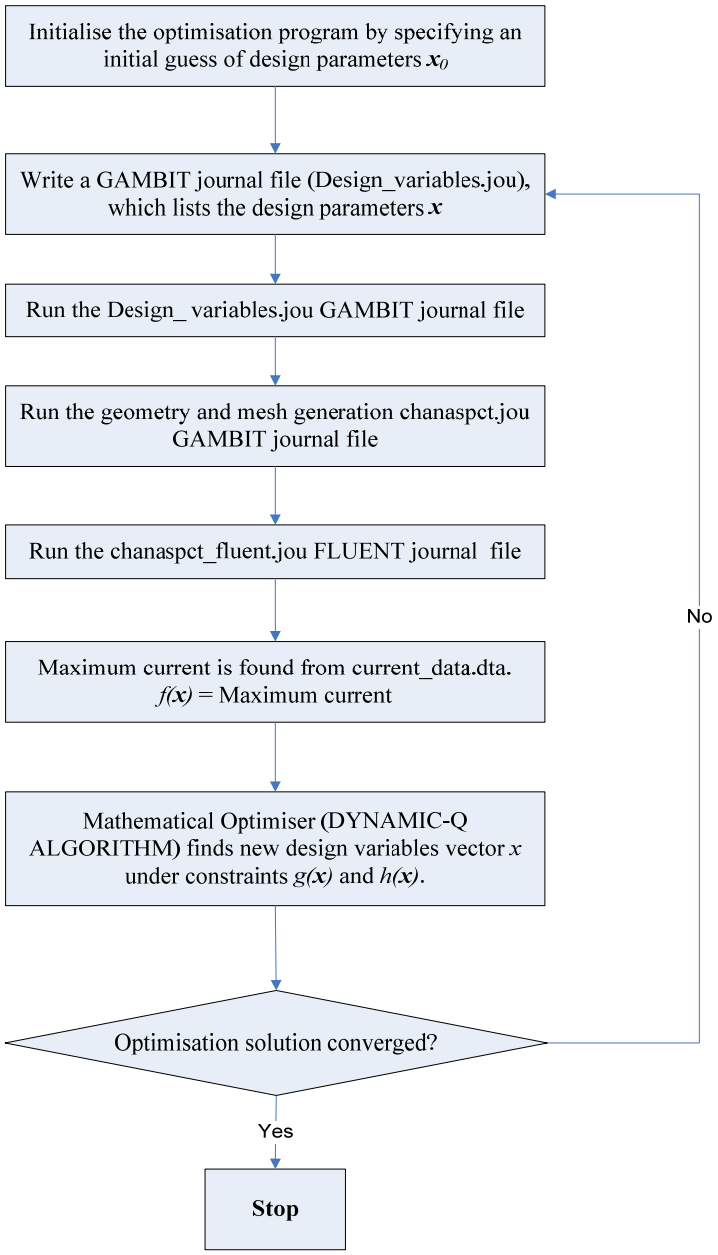

Figure 6.3 Optimisation automation flow diagram

6.5 RESULTS AND DISCUSSION

6.5.1 MODEL VALIDATION

In computational modelling, grid independence study and comparison of the CFD results with experimental data are the prescribed metrics for validation and verification of the CFD modelling studies. For fuel cell performance description, the polarisation or voltage-current (*IV*) curve is one of the most important final outcomes of numerical simulation and is widely used for validation purposes [193]. The simulation results for the base case operating conditions were verified against experimental measurements of Wang *et al.* [33]. The computed polarisation curve shown in Figure 6.4 is in good agreement with the experimental curves in the low load region. However, the model current density in the high mass transport limited region (> 1.5 A/cm^2) is higher than the experimental values. This might be due to possible experimental uncertainty or inadequate account of the effect of reduced oxygen transport, as a result of water flooding at the cathode side of the fuel cell at higher current density [150]. However, the predicted dependent variable distribution patterns could still be used successfully for better understanding of the complicated processes in fuel cell systems.

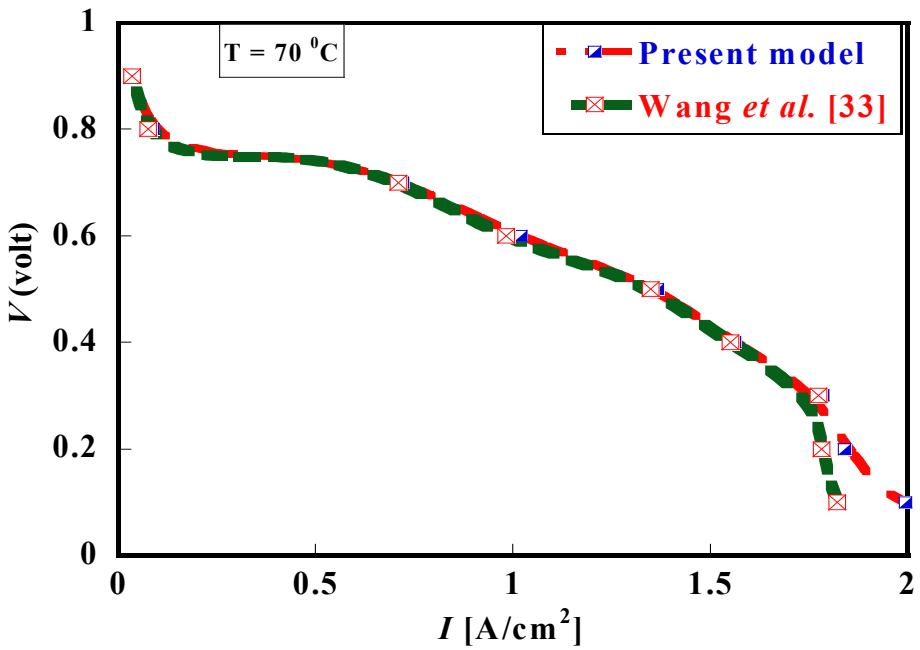

Figure 6.4 Comparison of numerical model prediction and experimental polarisation curves at base condition

6.5.2 PARAMETRIC STUDY RESULTS

In this section, a series of simulations was performed on a range of PEM fuel cell operating parameters to investigate their effect on the performance of the system. These parameters were investigated at operating cell voltage of 0.7 V and results are presented below.

First, the effect of temperature on the performance of a PEM fuel cell and the investigation of an optimal temperature range for the modelled PEM fuel cell system in this study is shown. Figure 6.5 shows the effect of an operating temperature from 50ºC to 90ºC on the performance of the PEM fuel cell system at steps of 10°C. The PEM fuel performance increase with the increase in cell temperature between 50ºC and 75ºC, since the water removal is easier and prevents incidence of flooding. The cell improvement at this temperature range is more noticeable at higher cell current

density. Meanwhile, an onset of decline in performance is observed as the operating temperature is increased beyond 75ºC. Profound performance deterioration occurred at temperatures between ≈75ºC and 90ºC, practically as a result of high membrane dehydration at these elevated temperatures.

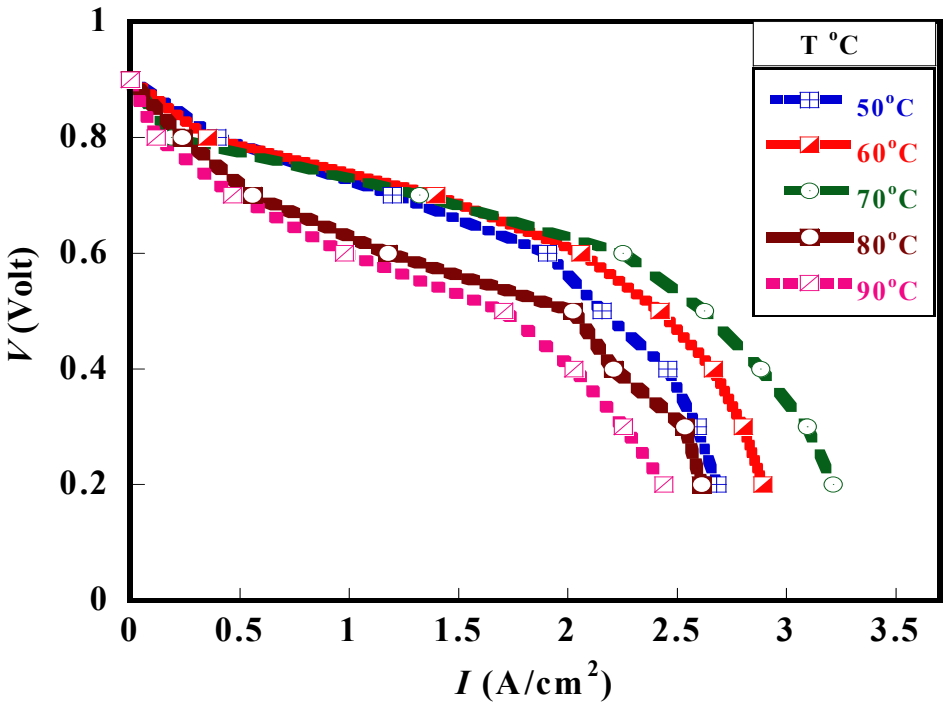

Figure 6.5 Effect of temperature on the PEM fuel cell performance at base conditions

Figure 6.6 clearly shows the optimal performance behaviour for the PEM fuel cell model and the point of decline of performance as the cell temperature increases beyond the optimal range level. This observed performance reduction phenomenon is a critical factor hindering the operation of PEM fuel cells beyond a certain temperature range to avoid fuel cell failure.

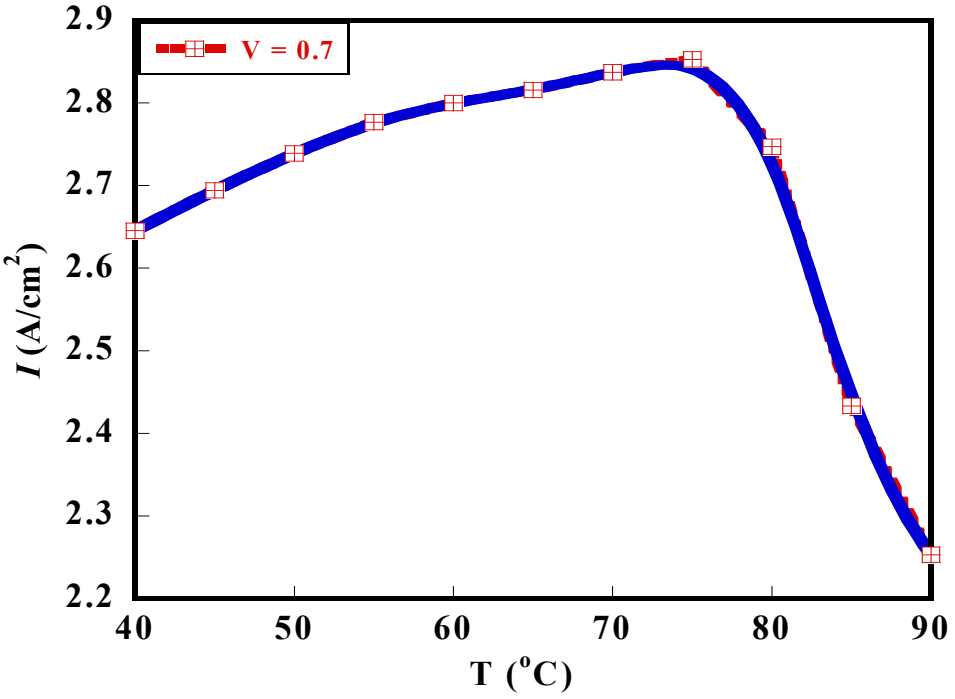

Figure 6.6 The cell current density as a function of temperature and the operating cell voltage

Figure 6.7 shows the polarisation curve at a varying stoichiometry number for a constant temperature (70°C) and pressure (P = 3 bar). For a low stoichiometry number, the removal of the cathode outlet flow decreases, thereby keeping the water concentration in the membrane layer increasing. This results in lower membrane resistance and subsequent lower ohmic over-potential, hence the improvement in cell performance. Meanwhile, at higher current density of the fuel cell, the low stoichiometry number adversely affects the cathode over-potential due to excessive resident water in the catalyst layer of the fuel cell system. Figure 6.8 depicts the PEM fuel cell behaviour at varying stoichiometry ratios of the cathode for three different current density loads. The figure shows that, at relatively low current density of the fuel cell system (0.42 A/cm^2), the air stoichiometry has little impact on the temperature.

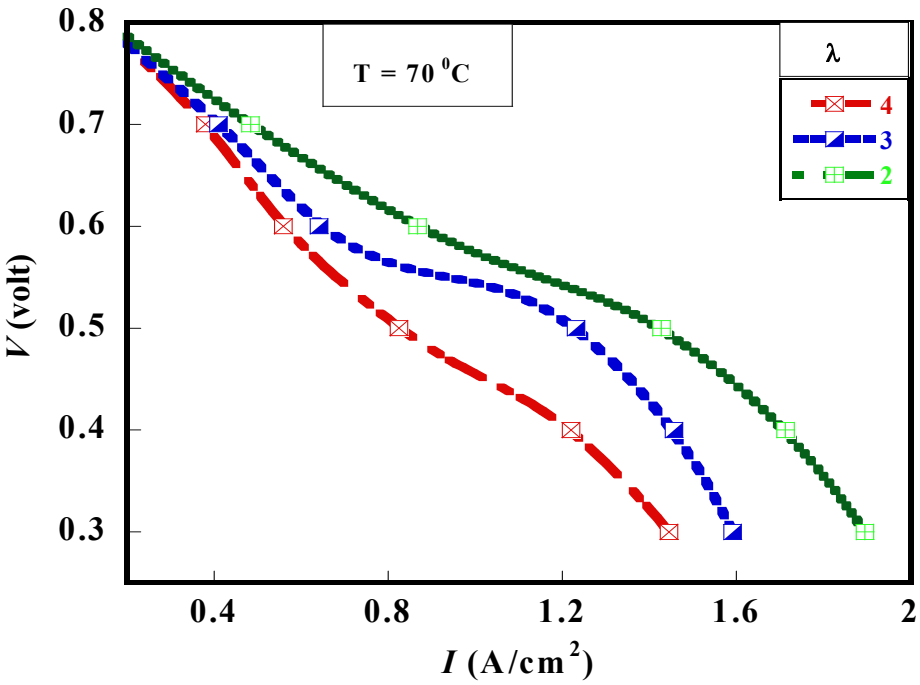

Figure 6.7 *I-V* curve at varying stoichiometry number. P = 3.0 bar and Re = 500

At this low current density, the rate of fuel consumption is small and the heat generation in the fuel cell system is minimal. For an increased current density (i.e. 0.72 A/cm^2) of the fuel cell system, which corresponds to higher reaction rates in the fuel cell system and subsequently increases in heat generation, the effect of the stoichiometry ratio becomes glaring on the cell temperature. The increased air stream improves heat transfer in the fuel cell system. This shows the possibility of an optimal match of temperature and stoichiometry ratio for improved fuel cell system performance.

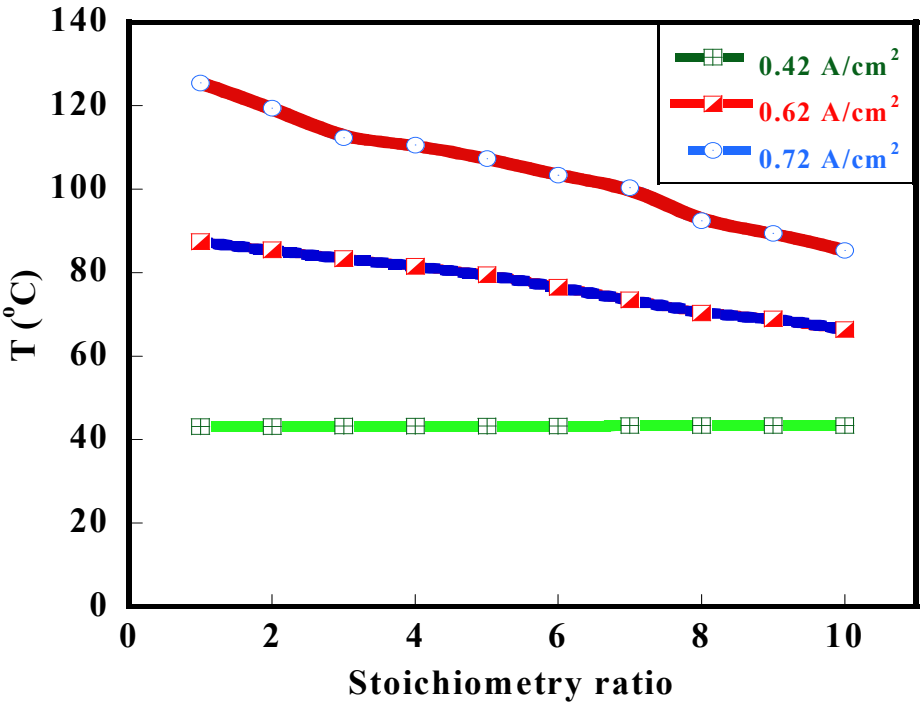

Figure 6.8 Effect of stoichiometry ratio on the PEM cell temperature at cell voltage of 0.7 V

Figure 6.9 shows the influence of relative humidity at the cathode inlet on the fuel cell output voltage. At an increased relative humidity at the cathode inlet, air transport to the catalyst is hindered. This results in an increase in the cathode over-potential, especially at a high operating current density of the fuel cell system. There is an increase in the generation of liquid water formation which results in reduced PEM fuel cell performance. This result shows that the relative humidity of the cathode inlet has a significant effect on liquid water formation and the extent of heat removal within the fuel cell system. For optimal system performance, this effect could be optimised in relation to other operating parameters.

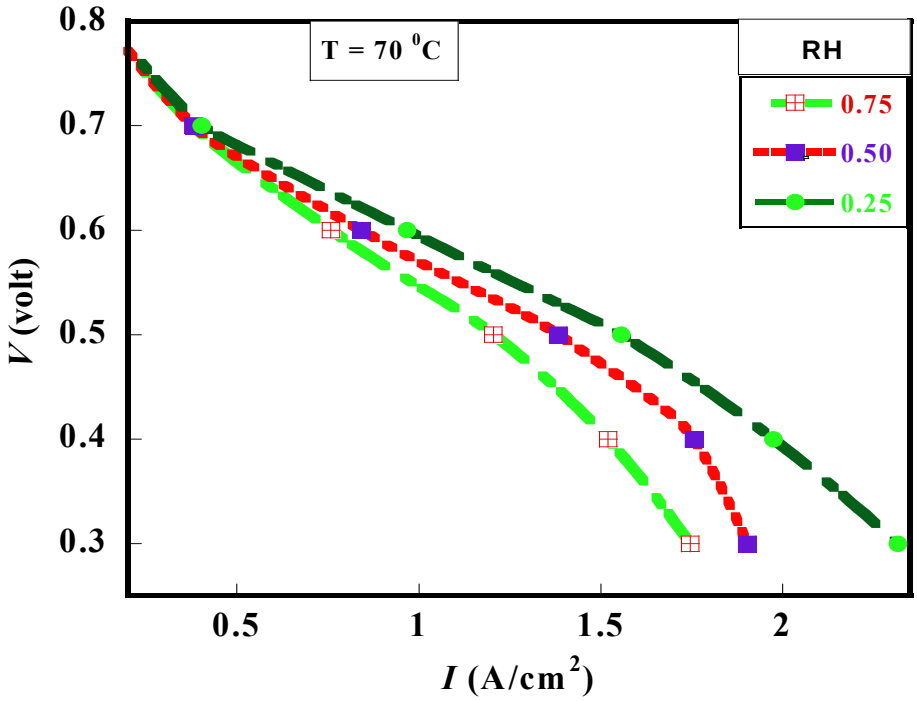

Figure 6.9 *I-V* curve at varying relative humidity (*RH*). *P* = 3.0 bar and Re = 500

Figure 6.10 shows the fuel cell performance at different aspect ratios of the cooling channels for a Reynolds number of 500. The result shows that fuel cell performance increases as the aspect ratio of the cooling channels increases to an operating temperature of 70ºC, until it reaches an optimal aspect ratio of ≈ 3.0 mm. Beyond the aspect ratio of about 3.0, cell performance starts to deplete. This result shows the existence of an optimal channel aspect ratio that optimises fuel cell performance in terms of current density. Figure 6.11 shows the *IV* curve for the cooling channel aspect ratios (Table 6.4) investigated at the base operating condition of the fuel cell. It is observed that fuel cell performance increases with the increase of the cooling channel aspect ratio at a cell operating temperature of 70°C. This increase in performance is likely due to an improvement in the cooling within the PEM fuel cell system, thereby increasing the cell membrane hydration and subsequently positively aiding cell performance.

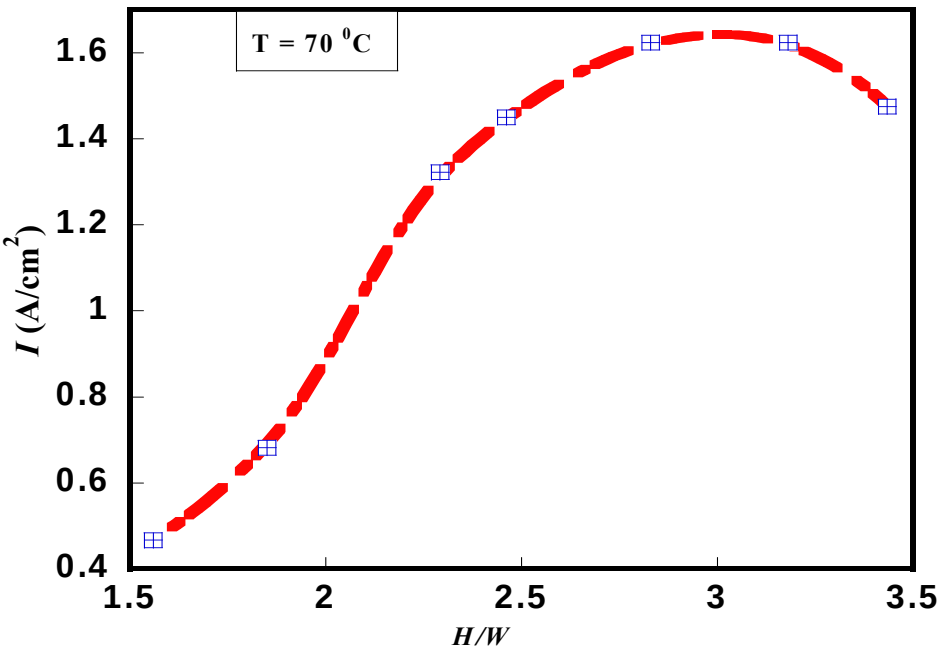

Figure 6.10 The cell current density at different aspect ratio at a cell potential of 0.7 V and a fixed Reynolds number of 500

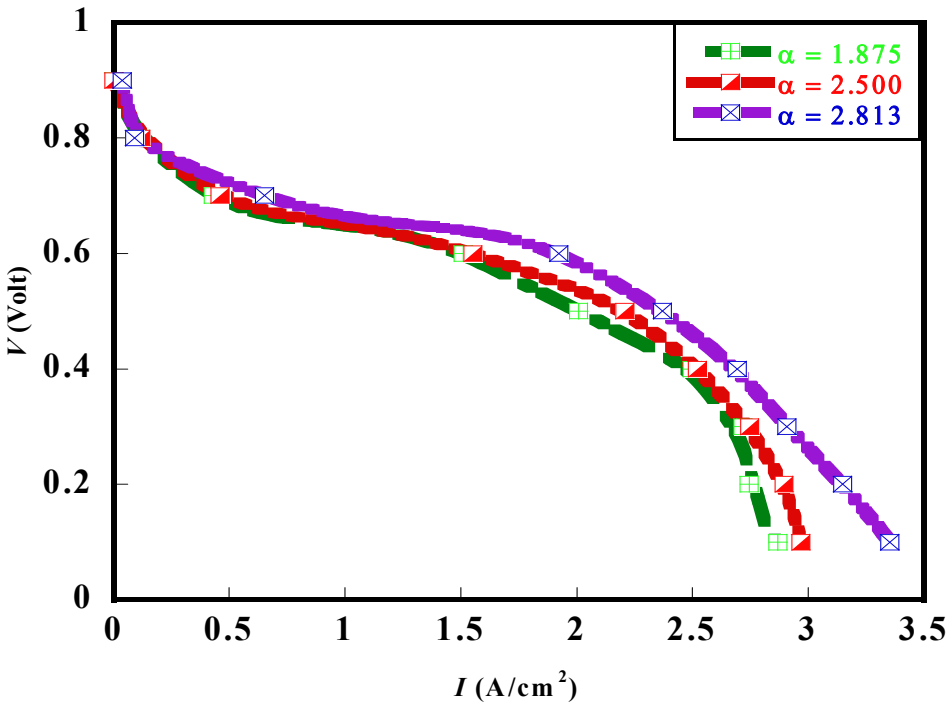

Figure 6.11 Current density at three cases of channel aspect ratio and Re = 500

6.5.3 OPTIMISATION RESULTS

The results obtained previously on the effect of the stoichiometry ratio, relative humidity and cooling channel aspect ratio on performance of the PEM fuel cells suggest the possibility of an optimal combination of these parameters for improved performance of PEM fuel cells when temperature is increased beyond the critical operating temperature which is typical of low temperature PEM fuel cells. Moreover, these factors are mutually dependent, especially in determining the rate of membrane hydration which, in turn, determines the reaction and transport characteristics in the fuel cell system. These factors are combined with varying cell operating temperatures to predict cell performance, especially when operation at higher temperatures (HT) is desired. It is well know that operating PEM fuel cells at higher operating temperatures eliminates some of the complications hindering improved performance. An intermediate HT-PEM (100-150°C) operating situation was investigated in this study. A series of numerical optimisations and calculations within the specified design constraint ranges in Section 6.4.1 were conducted to highlight the optimal

performance of the PEM fuel cell model studied in this work. Table 6.5 presents the obtained optimal values for the optimised parameters when using the Dynamic-Q algorithm.

Table 6.5 Values of optimised parameters

Model parameters	Optimised values (0.7V)
λ	4.161
RH	0.782
H/W	3.182

The maximised fuel cell performance was investigated at varying cell operating voltage for the combination of the optimal parameters in Table 6.5 at higher cell operating temperatures of the fuel cell. Table 6.6 shows the polarisation data based on the optimal design parameters for the different operating fuel cell voltages and temperatures.

Table 6.6 Polarisation data at optimised conditions and varying cell operating temperatures at Re = 500

Cell voltage (V)	I (A/cm^2) (T = 120 °C)	I (A/cm^2) (T = 130 °C)	I (A/cm^2) (T = 150 °C)
0.7	3.1421	3.6213	3.8228
0.6	4.0627	4.7341	5.1431
0.5	4.6814	5.4326	5.6314
0.4	5.3343	5.9531	6.3281

The results presented in Table 6.6 above shows that there is improvement in cell performance at different cell voltages with increasing cell operating temperatures. Higher performance was obtained al low cell operating voltages compared to higher cell voltages at different temperature ranges. The increase in cell current density difference was more prominent between the temperatures of 120°C and 130°C, but as

temperature increased towards 150°C, cell performance started to deplete negatively. When the operation was conducted beyond the 150°C level, the cell performance reduction became highly noticeable. This is most likely due to high level membrane dehydration beyond this temperature (150°C) level. The cooling to sustain the thermal build-up in the cell structure was no longer effective at this higher temperature level. Moreover, thermal stresses in PEM fuel cells are shown to rise as cell current density increases.

Figure 6.12 shows the peak current density as a function of cooling channel aspect ratio and cell temperature. An optimum cooling channel aspect ratio exists for the examined temperature ranges in which the peak fuel cell current density is maximised. This obtained result suggests that optimal arrangements of the channel geometry (aspect ratio), that could effectively maximise the cell current density of the fuel cell system, are feasible. In Figure 6.13, the optimal aspect ratio is shown as a function of the coolant Reynolds number and temperatures. The figure depicts an increase in the aspect ratio of the cooling channels as the Reynolds number increases from 100 to ≈ 300, but the rate of increment starts declining as the Reynolds number increases from 300.

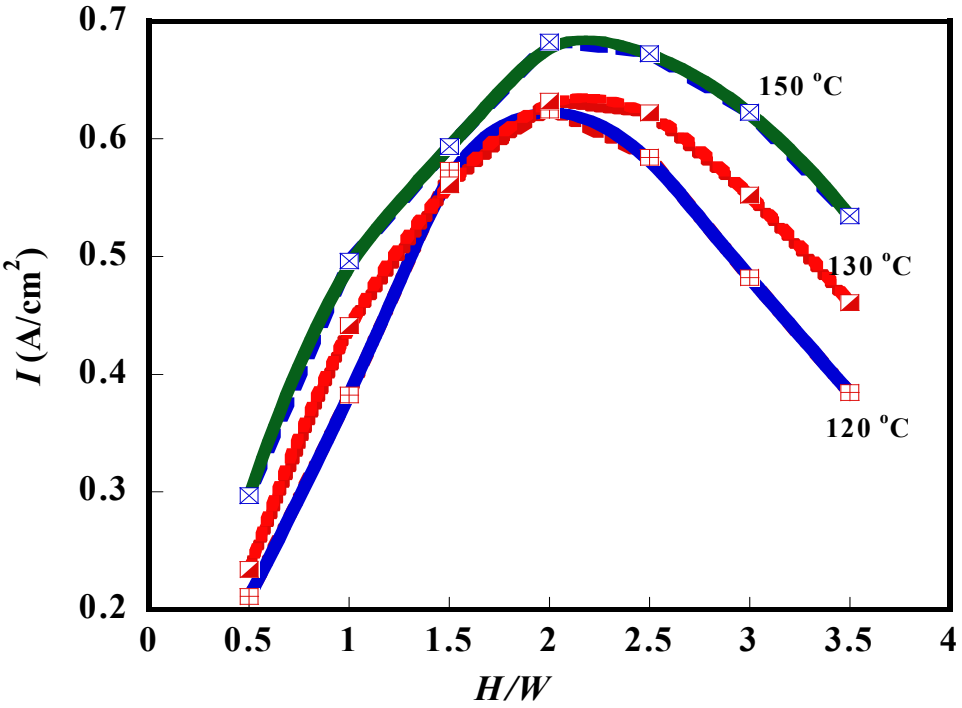

Figure 6.12 Effect of optimised cooling channel aspect ratio on the peak fuel cell current density at different temperatures and cell potential of 0.7V

The result further shows that, for an increased temperature to operate the fuel cell system, the required optimal aspect ratio increases, but at a relatively lower rate due to reduced system temperature as the coolant Reynolds number is increased. The result presented in Figure 6.13 can be correlated at temperature T = 110ºC by

$$\left(H/W\right)_{opt} = 2.22\,Re^{0.058} \quad . \tag{6.17}$$

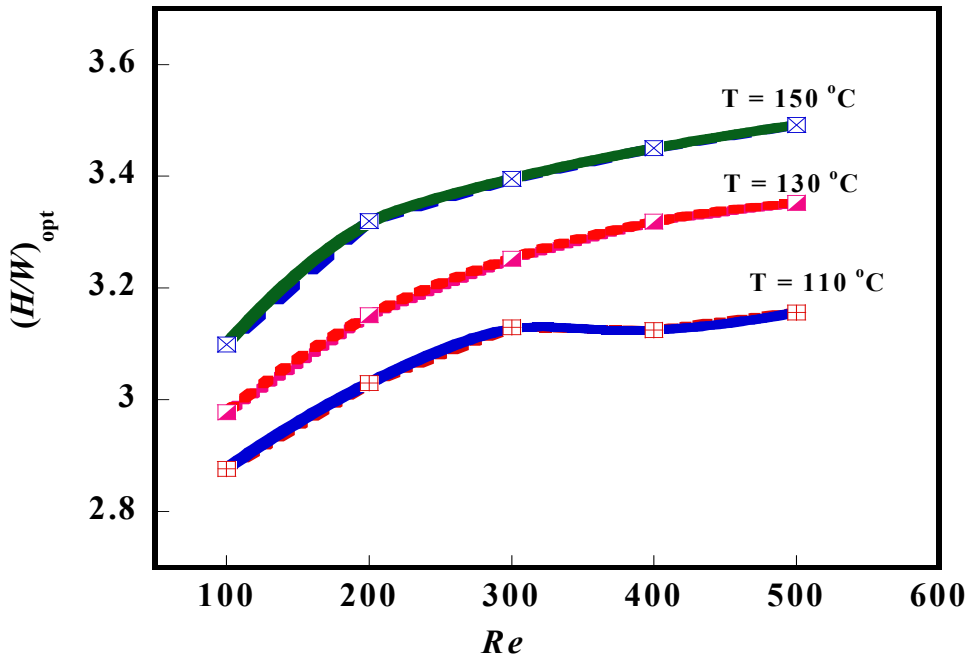

Figure 6.13 Effect of Reynolds number and temperature on the optimised aspect ratio of the cooling channel and cell potential of 0.7V

Figure 6.14 shows the effect of the maximised fuel cell current density as a function of the cooling gas Reynolds number for fixed cell temperatures and a fixed cooling channel aspect ratio of 2.50 mm. The maximised current density increases with an increase in the cooling channel Reynolds number. The result presented in Figure 6.14 can be correlated at temperature T = 130ºC by

$$I_{max} = 1.93\, Re^{0.092} \quad . \tag{6.18}$$

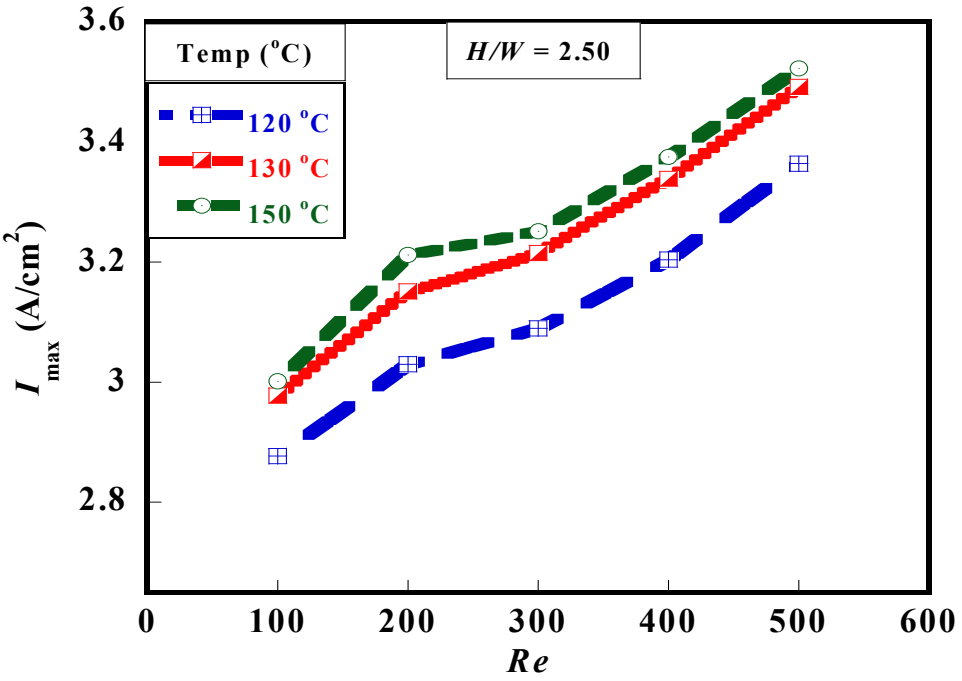

Figure 6.14 Effect of Reynolds number on the maximum current density at different cell temperatures and cell potential of 0.7V

In Figure 6.15, temperature contours on the membrane section of the fuel cell system are presented for varying cooling channel aspect ratios for a fuel cell voltage of 0.7 and a Reynolds number of 500. The result shows an improved temperature profile on the membrane section as the aspect ratio of the cooling channel increases for the examined cooling air Reynolds number.

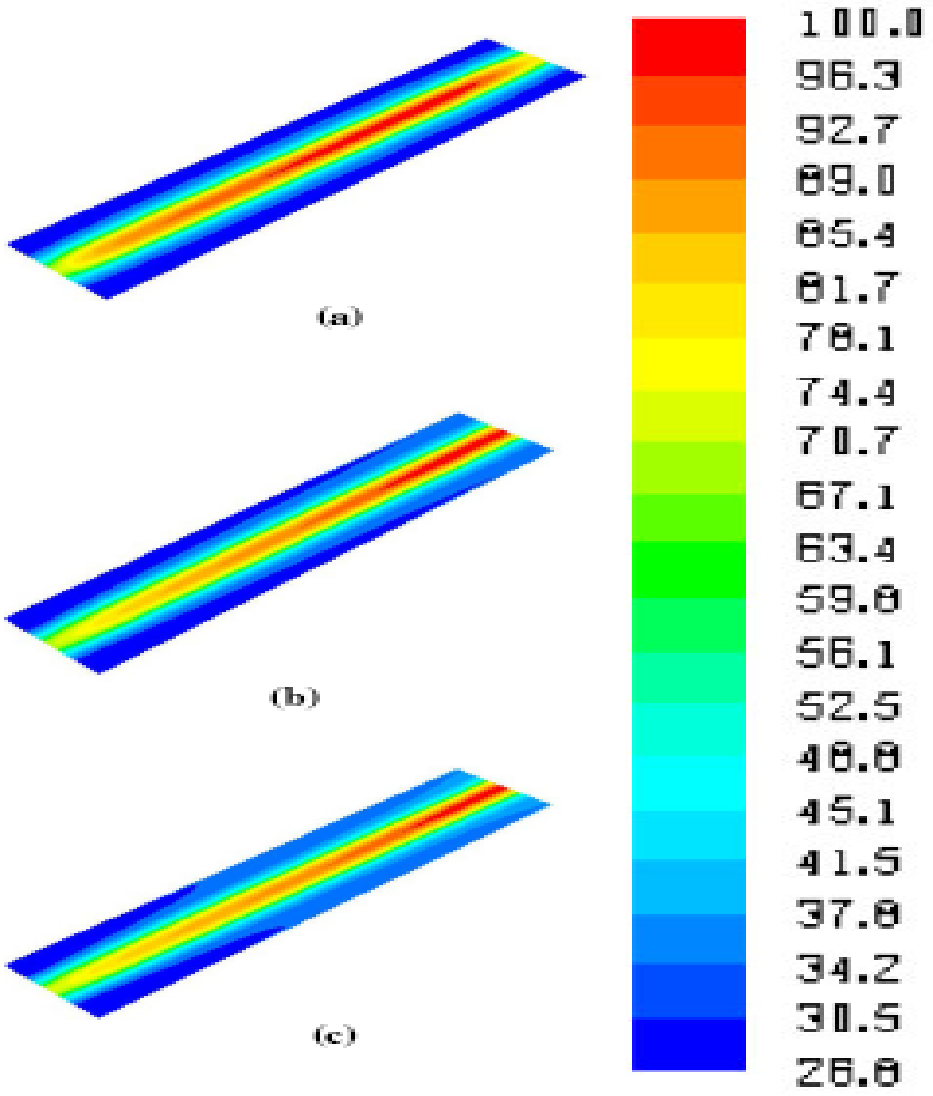

Figure 6.15 The local distribution of temperature along the membrane at different cooling channel aspect ratios and cell operating voltage of 0.7 V and Re = 500: (a) H/W = 1.875, (b) H/W = 2.500 and (c) H/W = 2.813

CONCLUSION

This chapter of the thesis is aimed at developing a numerical approach to improving PEM fuel cell performance at elevated operating temperatures through the combination of operating parameters with cooling channel aspect ratios. Numerical results indicate that operating parameters such as the stoichiometry ratio, relative

humidity and the cooling channel aspect ratio have a significant effect on fuel cell performance, primarily in determining the level of membrane dehydration of PEM fuel cells. Optimal values of the stoichiometry ratio, relative humidity and cooling channel aspect ratios were obtained by integrating a direct problem solver with an optimiser (Dynamic-Q). For the particular PEM fuel cell model operating conditions considered in this work, fuel cell performance is considerably enhanced when combining the studied parameters. Performance is more outstanding at temperatures between 120°C and 130°C. The performance increment then declines gradually from 130°C to 150°C. It should be noted that beyond 150°C, there is no significant increase in cell performance. The result of this work further shows that maximised current density also exist for varying cooling channel aspect ratios of the fuel cell system. The result also shows the possibility of operating low temperature PEM fuel cells beyond the typical critical temperatures ($\approx$ 75-80ºC), by using the combined optimal of the stoichiometry ratio, relative humidity and cooling channel geometry without the need for special temperature resistant materials for the PEM fuel cell. This study can easily be extended to varying cooling channel geometries and scaled for application in PEM stack systems for enhanced PEM fuel cell performance.

7

CHAPTER 7: CONCLUSIONS AND RECOMMENDATIONS

Although fossil fuel energy systems are affordable and widely available, they are finite and often accompanied by environmental pollution which has a negative impact on agriculture, health, social and the economic condition of the populace. Thus, the search for an alternative pollution-free affordable and widely-available energy source to replace the conventional fossil fuel has been receiving increased attention in the last decade. In this regard, the proton exchange membrane (PEM) fuel cell system has been touted to be one of the most promising clean and highly efficient power generation technologies of the future. In this thesis, factors that can enhance the performance of PEM fuel cell systems have been explored by using a combined numerical modelling and optimisation approach. The methodology developed in this work ensures an effective and accurate prediction of PEM fuel cell performance under different operating conditions. Novel approaches to performance enhancement were also introduced, especially in areas of reactant gas and thermal cooling optimisation for PEM fuel cells. The enhancement methodologies form the basis for new component geometry development that can be utilised to improve the advancement in system performance and manufacturing.

7.1 CONCLUSIONS

The major achievements and conclusions drawn from this study are summarised in the following.

(1) *Development of a finite-volume model to predict the performance of a PEM fuel cell system under different operating and design parameters:*

- This model highlights that temperature, GDL porosity, cathode gas mass flow rate and species flow orientation has significant impact on the performance of a PEM fuel cell.

- The model further shows that the impact of operating parameters on the performance of a PEM fuel cell is more significant at low operating cell voltages than at higher operating fuel cell voltages

- The results from the model underscore the interactive mutual interdependence of these fuel cell parameters during fuel cell operation and the need for an optimal match for these parameters for optimum fuel cell design.

(2) *Development of a finite-volume approach, combined with an optimisation algorithm to model reactant gas transport in a PEM fuel cell with a pin fin insert in the channel flow:*

- This model shows that performance in PEM fuel cells could be improved significantly by incorporating a pin fin in the channel flow. The Reynolds number had a significant effect on the diffusion of the reactant gas through the GDL medium.

- The fuel channel friction factor also increased with an increase in the clearance ratio of the pin fin while it decreased with an increasing GDL porosity. Hence, the channel friction and pressure drop can be reduced significantly with the increasing GDL porosity, though at an optimal value.

- The optimal clearance ratio and pitch for the considered fuel cell channel

decreased with an increase in the fuel channel friction factor. Optimal pin fin clearance ratio exists which offered a minimum pumping power requirement.

(3) *Development of a finite-volume approach, combined with an optimisation algorithm to model the impact of cooling channel geometry on the thermal management and performance of a PEM fuel cell system:*

- The results from this model show that fuel cell performance is considerably enhanced when PEM fuel cells operate at combined optimised design parameters. Performance is more outstanding at temperatures between 120°C and 130°C. However, the performance increment rate declines gradually from 130°C to 150°C.

- The result of this study shows the possibility of operating a PEM fuel cell beyond the critical temperature range (≤ 80°C) by using the combined optimised stoichiometry ratio, relative humidity and cooling channel geometry, without the need for special temperature resistant materials for the PEM fuel cell which constitute additional cost for PEM fuel cell development.

- It should also be noted that this study can easily be extended to different cooling channels (apart from the rectangular channels used in this study) in order to enhance the performance of PEM fuel.

In summary, this research work has shown the feasibility of designing fuel cells with enhanced performance by using only the CFD approach or this approach in combination with an optimiser. The use of the CFD approach alone provides improvement in the lead time reduction for PEM fuel cell system development when compared with development based solely on an experimental method (design and test approach). However, the obtained results are not usually a distinct optimum for system design. An optimiser such as the Dynamic-Q combined with the CFD codes

show a more robust and distinct optimal result that is more accurate and suitable for implementation during system design. Furthermore, it should be stressed that there is a need for proper understanding of the problem formulation and implementation of the modelling approach for a successful outcome, especially when combining the CFD codes with the optimisation algorithm. This hinges more on the modelling skill, expertise and experience of the modeller. The modelling methodology implemented in this thesis can be applied to other fuel cell system designs (such as Solid oxide fuel cell structure), provided a proper problem formulation is implemented. Also, scaling of the obtained results in this research work is practicable for large scale PEM fuel cell stack system design.

7.2 RECOMMENDATIONS

The numerical methodologies and models presented in this research work could be further improved and/or extended in the following directions:

- In the models presented in this thesis, assumptions of isotropic and homogeneous properties of the porous medium were applied. There is a need to evaluate PEM fuel cell system performance under different material properties of the porous medium, including the catalyst.

- In real PEM fuel cell system operation, the incidences of two-phase flow of liquid in the channel structure are inevitable and have significant impact on fuel cell performance. The physics governing the model could be improved in order to increase the applicability of this model by extension to two-phase capability.

- In modelling the phase change of liquid water, the assumptions of evaporation and condensation rate constants are commonly used. More detailed models on system performance should incorporate a functional dependence of evaporation and condensation rates rather than a constant value.

- In terms of computational complexity, large scale simulation using parallel computing will reduce the computational time, especially in such models as presented in this thesis, where multi-parameter evaluation, which combines CFD with an optimisation algorithm, is involved.

- In computational fuel cell models, such as the ones presented in this research, there is a need to validate the results against adequate experimental data. Future work should involve the design of modelled systems studied on standard fuel cell test stations. This will ensure adequate validity and implementation of model results in the PEM development process.